
Solution of a Semicoercive Variational Inequality

by TFETI Method

To give an example of a class of bound and equality constrained problems with uniformly bounded spectrum arising in important applications, let us consider the solution of the discretized elliptic semicoercive variational inequalities, such as those describing the equilibrium of a system of elastic bodies in mutual unilateral frictionless contact in case that some bodies are not sufficiently fixed along the boundary. The presence of “floating” bodies is a considerable complication as the corresponding stiffness matrices are singular. To simplify our exposition, we again restrict our attention to a model variational inequality governed by the Laplace operator on 2D domains.

Our main tool is a variant of the classical FETI method called total FETI (TFETI), which was proposed independently by Dostál, Horák, and Kučera [68] and Of (all floating FETI) [156] as a parallel solver for the problems described by elliptic partial differential equations. The TFETI method differs from the original FETI method in the way which is used to implement the Dirichlet boundary conditions. While the FETI method assumes that the subdomains inherit the Dirichlet boundary conditions from the original problem, TFETI uses the Lagrange multipliers to “glue” the subdomains to the boundary whenever the Dirichlet boundary conditions are prescribed. Such approach simplifies the implementation as all the stiffness matrices of the subdomains have typically a priori known kernels and can be treated in the same way. Moreover, the kernels can be used for effective evaluation of the action of a generalized inverse by means of Lemma 1.1. The procedure can be naturally combined with the preconditioning by the “natural coarse grid” introduced by Farhat, Mandel, and Roux [85]. This preconditioning results in the class of problems with the condition number of the regular part of the Hessian matrix bounded by CH/h , where C , H , and h are a constant, decomposition, and discretization parameters, respectively. This compares favorably with the estimate CH^2/h^2 of Proposition 7.1 for non-preconditioned FETI–DP. Here we use the duality theory of Sect. 2.6.5 and Theorem 6.11 to modify the TFETI method for the solution of variational inequalities.

8.1 Model Semicoercive Variational Inequality

Let $\Omega = \Omega^1 \cup \Omega^2$, where $\Omega^1 = (0, 1) \times (0, 1)$ and $\Omega^2 = (1, 2) \times (0, 1)$ denote open domains with boundaries Γ^1, Γ^2 and their parts Γ_u^i, Γ_f^i , and Γ_c^i formed by the sides of $\Omega^i, i = 1, 2$.

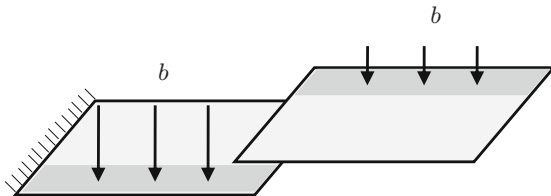


Fig. 8.1. Semicoercive model problem

Let $H^1(\Omega^i), i = 1, 2$, denote the Sobolev space of the first order in the space $L^2(\Omega^i)$ of the functions on Ω^i whose squares are integrable in the sense of Lebesgue. Let

$$\mathcal{V}^i = \{v^i \in H^1(\Omega^i) : v^i = 0 \text{ on } \Gamma_u^i\}$$

denote the closed subspaces of $H^1(\Omega^i), i = 1, 2$, and let

$$\mathcal{V} = \mathcal{V}^1 \times \mathcal{V}^2 \quad \text{and} \quad \mathcal{K} = \{(v^1, v^2) \in \mathcal{V} : v^2 - v^1 \geq 0 \text{ on } \Gamma_c\}$$

denote the closed subspace and the closed convex subset of

$$\mathcal{H} = H^1(\Omega^1) \times H^1(\Omega^2),$$

respectively. The relations on the boundaries are in terms of traces. We shall define on \mathcal{H} the symmetric bilinear form

$$a(u, v) = \sum_{i=1}^2 \int_{\Omega^i} \left(\frac{\partial u^i}{\partial x} \frac{\partial v^i}{\partial x} + \frac{\partial u^i}{\partial y} \frac{\partial v^i}{\partial y} \right) d\Omega$$

and the linear form

$$b(v) = \sum_{i=1}^2 \int_{\Omega^i} b^i v^i d\Omega,$$

where $b^i \in L^2(\Omega^i), i = 1, 2$ are the restrictions of

$$b(x, y) = \begin{cases} -3 & \text{for } (x, y) \in (0, 1) \times [0.75, 1), \\ 0 & \text{for } (x, y) \in (0, 1) \times [0, 0.75) \quad \text{and} \quad (x, y) \in (1, 2) \times [0.25, 1), \\ -1 & \text{for } (x, y) \in (1, 2) \times [0, 0.25). \end{cases}$$

Denoting for each $u \in \mathcal{H}$

$$f(u) = \frac{1}{2}a(u, u) - b(u) = \frac{1}{2} \sum_{i=1}^2 \int_{\Omega^i} \|\nabla u^i\|^2 d\Omega - \sum_{i=1}^2 \int_{\Omega^i} b^i v^i d\Omega,$$

we can define the continuous problem to find

$$\min_{u \in \mathcal{K}} f(u). \tag{8.1}$$

The solution of the model problem can be interpreted as the displacement of two membranes under the traction b as in Fig. 8.1. The left edge of the right membrane is not allowed to penetrate below the right edge of the left membrane. Notice that only the left membrane is fixed on the outer edge and the right membrane has no prescribed displacement, so that

$$\Gamma_u^1 = \{(0, y) \in \mathbb{R}^2 : y \in [0, 1]\}, \quad \Gamma_u^2 = \emptyset.$$

Even though the form a is only semicoercive, the form b is still coercive due to the choice of b so that it has a unique solution [120, 99].

8.2 TFETI Domain Decomposition and Discretization

In our definition of the problem, we have so far used only the natural decomposition of the spatial domain Ω into Ω^1 and Ω^2 . To enable efficient application of the domain decomposition methods, we decompose each Ω^i into subdomains $\Omega^{i1}, \dots, \Omega^{ip}$, $p > 1$, as in Fig. 8.2.

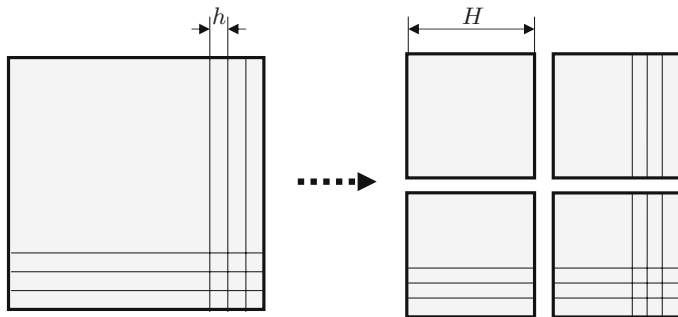


Fig. 8.2. Domain decomposition and discretization

The continuity of the global solution in Ω^1 and Ω^2 is enforced by the “gluing” conditions $u^{ij}(\mathbf{X}) = u^{ik}(\mathbf{X})$ that should be satisfied for any point \mathbf{X} on the interface $\Gamma^{ij,ik}$ of Ω^{ij} and Ω^{ik} .

After modifying appropriately the definition of problem (8.1), introducing regular grids in the subdomains Ω^{ij} that match across the interfaces $\Gamma^{ij,kl}$,

indexing contiguously the nodes and entries of corresponding vectors in the subdomains, and using the Lagrangian finite element discretization, we get the discretized version of problem (8.1) with auxiliary domain decomposition that reads

$$\min \frac{1}{2} \mathbf{x}^T \mathbf{A} \mathbf{x} - \mathbf{b}^T \mathbf{x} \quad \text{s.t.} \quad \mathbf{B}_{\mathcal{I}^*} \mathbf{x} \leq \mathbf{o} \quad \text{and} \quad \mathbf{B}_{\mathcal{E}^*} \mathbf{x} = \mathbf{o}. \quad (8.2)$$

In (8.2), the Hessian matrix

$$\mathbf{A} = \begin{bmatrix} \mathbf{A}_1 & \mathbf{O} & \dots & \mathbf{O} \\ \mathbf{O} & \mathbf{A}_2 & \dots & \mathbf{O} \\ \vdots & \vdots & \dots & \vdots \\ \mathbf{O} & \mathbf{O} & \dots & \mathbf{A}_{2p} \end{bmatrix}$$

is a block diagonal positive semidefinite stiffness matrix. The diagonal blocks \mathbf{A}_i are the local stiffness matrices of the subdomains with the same kernel; for $j = 1, 2$ and $k = 1, \dots, p$, the matrix $\mathbf{A}_{p(j-1)+k}$ corresponds to the subdomain Ω^{jk} . If the nodes in each subdomain are ordered columnwise, the blocks \mathbf{A}_i are band matrices.

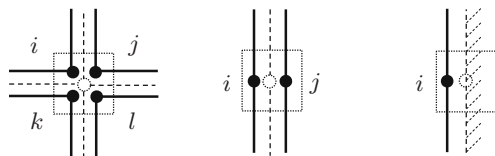


Fig. 8.3. Three types of constraints

The full rank matrices $\mathbf{B}_{\mathcal{I}^*}$ and $\mathbf{B}_{\mathcal{E}^*}$ describe the discretized nonpenetration and gluing conditions, respectively, and \mathbf{b} represents the discrete analog of the linear term $b(u)$. The rows of $\mathbf{B}_{\mathcal{E}^*}$ and $\mathbf{B}_{\mathcal{I}^*}$ are filled with zeros except 1 and -1 in the positions that correspond to the nodes with the same coordinates on the artificial or contact boundaries, respectively. If \mathbf{b}_i denotes a row of $\mathbf{B}_{\mathcal{E}^*}$ or $\mathbf{B}_{\mathcal{I}^*}$, then \mathbf{b}_i does not have more than four nonzero entries. The continuity of the solution in the “wire basket” comprising the nodes with indices i, j, k, l (see Fig. 8.3 left) is enforced by the equalities

$$x_i = x_j, \quad x_k = x_l, \quad x_i + x_j = x_k + x_l,$$

which can be expressed by the vectors

$$\mathbf{b}_{ij} = (\mathbf{s}_i - \mathbf{s}_j)^T, \quad \mathbf{b}_{kl} = (\mathbf{s}_k - \mathbf{s}_l)^T, \quad \mathbf{b}_{ijkl} = (\mathbf{s}_i + \mathbf{s}_j - \mathbf{s}_k - \mathbf{s}_l)^T,$$

where \mathbf{s}_i denotes the i th column of the identity matrix \mathbf{I}_n . The continuity of the solution across the subdomains interface (see Fig. 8.3 middle) is implemented

by $\mathbf{b}_{ij}\mathbf{x} = 0$ as in the FETI-DP method discussed in Sect. 7.2, so that $\mathbf{b}_{ij}\mathbf{x}$ denotes the jump across the boundary, and the Dirichlet boundary condition (see Fig. 8.3 right) $x_i = 0$ is implemented by the row $\mathbf{b}_i = \mathbf{s}_i^T$.

Our next step is to simplify the problem, in particular to replace the general inequality constraints $\mathbf{B}_{\mathcal{I}}\mathbf{x} \leq \mathbf{o}$ by the nonnegativity constraints using the duality theory. To this end, let us denote the Lagrange multipliers associated with the inequality and equality constraints of problem (8.2) by $\boldsymbol{\lambda}_{\mathcal{I}}$ and $\boldsymbol{\lambda}_{\mathcal{E}}$, respectively, and assume that the rows of \mathbf{B} are ordered in such a way that

$$\boldsymbol{\lambda} = \begin{bmatrix} \boldsymbol{\lambda}_{\mathcal{I}} \\ \boldsymbol{\lambda}_{\mathcal{E}} \end{bmatrix} \quad \text{and} \quad \mathbf{B} = \begin{bmatrix} \mathbf{B}_{\mathcal{I}} \\ \mathbf{B}_{\mathcal{E}} \end{bmatrix}.$$

We formed \mathbf{B} in such a way that it is a full rank matrix. Finally, let \mathbf{R} denote the full column rank matrix whose columns span $\text{Ker}\mathbf{A}$. Then we can use Proposition 2.22 to get that the Lagrange multipliers $\boldsymbol{\lambda}$ for problem (8.2) solve the constrained dual problem

$$\max \Theta(\boldsymbol{\lambda}) \quad \text{s.t.} \quad \boldsymbol{\lambda}_{\mathcal{I}} \geq \mathbf{o} \quad \text{and} \quad \mathbf{R}^T(\mathbf{b} - \mathbf{B}^T\boldsymbol{\lambda}) = \mathbf{o},$$

where $\Theta(\boldsymbol{\lambda})$ is the dual function. Changing the signs of Θ and discarding the constant term, we get that the Lagrange multipliers $\boldsymbol{\lambda}$ solve the bound and equality constrained problem

$$\min \theta(\boldsymbol{\lambda}) \quad \text{s.t.} \quad \boldsymbol{\lambda}_{\mathcal{I}} \geq \mathbf{o} \quad \text{and} \quad \mathbf{R}^T(\mathbf{b} - \mathbf{B}^T\boldsymbol{\lambda}) = \mathbf{o}, \tag{8.3}$$

where

$$\theta(\boldsymbol{\lambda}) = \frac{1}{2}\boldsymbol{\lambda}^T\mathbf{B}\mathbf{A}^+\mathbf{B}^T\boldsymbol{\lambda} - \boldsymbol{\lambda}^T\mathbf{B}\mathbf{A}^+\mathbf{b}$$

and \mathbf{A}^+ is any symmetric positive semidefinite generalized inverse. In our computations, we use the generalized inverse $\mathbf{A}^\#$ defined by (1.7).

Notice that using the block diagonal and band structure of \mathbf{A} together with

$$\text{Ker}\mathbf{A}_i = [1, \dots, 1]^T, \quad i = 1, \dots, 2p,$$

we can effectively evaluate $\mathbf{A}^\#\mathbf{y}$ for any $\mathbf{y} \in \mathbb{R}^n$. Indeed, using the Cholesky decomposition described in Sect. 1.5, we get the lower triangular band matrices \mathbf{L}_i such that $\mathbf{A}_i = \mathbf{L}_i\mathbf{L}_i^T$. Since $\mathbf{A}_i^\# = (\mathbf{L}_i^\#)^T\mathbf{L}_i^\#$ and

$$\mathbf{A}^\# = \text{diag}(\mathbf{A}_1^\#, \mathbf{A}_2^\#, \dots, \mathbf{A}_{2p}^\#),$$

we get

$$\mathbf{A}^\#\mathbf{y} = \sum_{i=1}^{2p} \mathbf{A}_i\mathbf{y}_i = \sum_{i=1}^{2p} (\mathbf{L}_i^\#)^T(\mathbf{L}_i^\#\mathbf{y}_i),$$

where we assume that the decomposition $\mathbf{y}^T = [\mathbf{y}_1^T, \mathbf{y}_2^T, \dots, \mathbf{y}_{2p}^T]$ complies with the block structure of \mathbf{A} . If the dimension of the blocks \mathbf{A}_i is uniformly bounded, then the computational cost increases nearly proportionally to p . Moreover, the time that is necessary for the decomposition $\mathbf{A} = \mathbf{L}\mathbf{L}^T$ and evaluation of $(\mathbf{L}^\#)^T\mathbf{L}^\#\mathbf{y}$ can be reduced nearly proportionally by parallel implementation.

8.3 Natural Coarse Grid

Even though problem (8.3) is much more suitable for computations than (8.2), further improvement may be achieved by adapting some simple observations and the results of Farhat, Mandel, and Roux [85]. Let us denote

$$\begin{aligned} \mathbf{F} &= \mathbf{B}\mathbf{A}^+\mathbf{B}^T, & \tilde{\mathbf{d}} &= \mathbf{B}\mathbf{A}^T\mathbf{b}, \\ \tilde{\mathbf{G}} &= \mathbf{R}^T\mathbf{B}^T, & \tilde{\mathbf{e}} &= \mathbf{R}^T\mathbf{b}, \end{aligned}$$

and let \mathbf{T} denote a regular matrix that defines orthonormalization of the rows of $\tilde{\mathbf{G}}$ so that the matrix

$$\mathbf{G} = \mathbf{T}\tilde{\mathbf{G}}$$

has orthonormal rows. After denoting

$$\mathbf{e} = \mathbf{T}\tilde{\mathbf{e}},$$

problem (8.3) reads

$$\min \frac{1}{2}\boldsymbol{\lambda}^T\mathbf{F}\boldsymbol{\lambda} - \boldsymbol{\lambda}^T\tilde{\mathbf{d}} \quad \text{s.t.} \quad \boldsymbol{\lambda}_{\mathcal{I}} \geq \mathbf{o} \quad \text{and} \quad \mathbf{G}\boldsymbol{\lambda} = \mathbf{e}. \quad (8.4)$$

Next we shall transform the problem of minimization on the subset of the affine space to that on the subset of the vector space by looking for the solution of (8.4) in the form $\boldsymbol{\lambda} = \boldsymbol{\mu} + \tilde{\boldsymbol{\lambda}}$, where $\mathbf{G}\tilde{\boldsymbol{\lambda}} = \mathbf{e}$. The following lemma shows that we can even find $\tilde{\boldsymbol{\lambda}}$ such that $\tilde{\boldsymbol{\lambda}}_{\mathcal{I}} = \mathbf{o}$.

Lemma 8.1. *Let \mathbf{B} be such that the negative entries of $\mathbf{B}_{\mathcal{I}}$ are in the columns that correspond to the nodes in the floating subdomain Ω^2 . Then there is $\tilde{\boldsymbol{\lambda}}_{\mathcal{I}}$ such that $\tilde{\boldsymbol{\lambda}}_{\mathcal{I}} \geq \mathbf{o}$ and $\mathbf{G}\tilde{\boldsymbol{\lambda}} = \tilde{\mathbf{e}}$.*

Proof. See [65]. □

To carry out the transformation, substitute $\boldsymbol{\lambda} = \boldsymbol{\mu} + \tilde{\boldsymbol{\lambda}}$ to get

$$\frac{1}{2}\boldsymbol{\lambda}^T\mathbf{F}\boldsymbol{\lambda} - \boldsymbol{\lambda}^T\tilde{\mathbf{d}} = \frac{1}{2}\boldsymbol{\mu}^T\mathbf{F}\boldsymbol{\mu} - \boldsymbol{\mu}^T(\tilde{\mathbf{d}} - \mathbf{F}\tilde{\boldsymbol{\lambda}}) + \frac{1}{2}\tilde{\boldsymbol{\lambda}}^T\mathbf{F}\tilde{\boldsymbol{\lambda}} - \tilde{\boldsymbol{\lambda}}^T\tilde{\mathbf{d}}.$$

After returning to the old notation, problem (8.4) is reduced to

$$\min \frac{1}{2}\boldsymbol{\lambda}^T\mathbf{F}\boldsymbol{\lambda} - \boldsymbol{\lambda}^T\mathbf{d} \quad \text{s.t.} \quad \mathbf{G}\boldsymbol{\lambda} = \mathbf{o} \quad \text{and} \quad \boldsymbol{\lambda}_{\mathcal{I}} \geq -\tilde{\boldsymbol{\lambda}}_{\mathcal{I}} \quad (8.5)$$

with $\mathbf{d} = \tilde{\mathbf{d}} - \mathbf{F}\tilde{\boldsymbol{\lambda}}$ and $\tilde{\boldsymbol{\lambda}}_{\mathcal{I}} \geq \mathbf{o}$.

Our final step is based on the observation that (8.5) is equivalent to

$$\min \frac{1}{2}\boldsymbol{\lambda}^T(\mathbf{P}\mathbf{F}\mathbf{P} + \bar{\rho}\mathbf{Q})\boldsymbol{\lambda} - \boldsymbol{\lambda}^T\mathbf{P}\mathbf{d} \quad \text{s.t.} \quad \mathbf{G}\boldsymbol{\lambda} = \mathbf{o} \quad \text{and} \quad \boldsymbol{\lambda}_{\mathcal{I}} \geq -\tilde{\boldsymbol{\lambda}}_{\mathcal{I}}, \quad (8.6)$$

where $\bar{\varrho}$ is an arbitrary positive constant and

$$Q = G^T G \quad \text{and} \quad P = I - Q$$

denote the orthogonal projectors on the image space of G^T and on the kernel of G , respectively. The regularization term is introduced in order to simplify the reference to the results of quadratic programming that assume regularity of the Hessian matrix of the quadratic form. Problem (8.6) turns out to be a suitable starting point for development of an efficient algorithm for variational inequalities due to the following classical estimates of the extreme eigenvalues.

Theorem 8.2. *There are constants $C_1 > 0$ and $C_2 > 0$ independent of the discretization parameter h and the decomposition parameter H such that*

$$C_1 \leq \lambda_{\min}(\text{PFP}|\text{Im}P) \quad \text{and} \quad \lambda_{\max}(\text{PFP}|\text{Im}P) \leq \|\text{PFP}\| \leq C_2 \frac{H}{h},$$

where λ_{\min} and λ_{\max} denote the corresponding extremal eigenvalues of corresponding matrices.

Proof. See Theorem 3.2 of Farhat, Mandel, and Roux [85]. Let us point out that the statement of Theorem 3.2 of Farhat, Mandel and Roux [85] gives only an upper bound on the spectral condition number $\kappa(\text{PFP}|\text{Im}P)$, but the reasoning that precedes and substantiates their estimate proves both bounds of (8.2). □

8.4 Optimality

To show that Algorithm 6.1 with the inner loop implemented by Algorithm 5.8 is optimal for the solution of problem (or a class of problems) (8.6), let us introduce new notation that complies with that used to define the class of problems (6.34) introduced in Sect. 6.7.

As in Chap. 7, we use

$$\mathcal{T} = \{(H, h) \in \mathbb{R}^2 : H \leq 1, 0 < 2h \leq H, \text{ and } H/h \in \mathbb{N}\}$$

as the set of indices, where \mathbb{N} denotes the set of all positive integers. Given a constant $C \geq 2$, we shall define a subset \mathcal{T}_C of \mathcal{T} by

$$\mathcal{T}_C = \{(H, h) \in \mathcal{T} : H/h \leq C\}.$$

For any $t \in \mathcal{T}$, we shall define

$$\begin{aligned} A_t &= \text{PFP} + \bar{\varrho}Q, & \mathbf{b}_t &= P\mathbf{d} \\ B_t &= G, & \ell_{t,\mathcal{I}} &= -\tilde{\lambda}_{\mathcal{I}} \text{ and } \ell_{t,\mathcal{E}} = -\infty \end{aligned}$$

by the vectors and matrices generated with the discretization and decomposition parameters H and h , respectively, so that problem (8.6) is equivalent to the problem

$$\text{minimize } f_t(\boldsymbol{\lambda}_t) \text{ s.t. } \mathbf{C}_t \boldsymbol{\lambda}_t = \mathbf{o} \text{ and } \boldsymbol{\lambda}_t \geq \boldsymbol{\ell}_t \tag{8.7}$$

with $f_t(\boldsymbol{\lambda}) = \frac{1}{2} \boldsymbol{\lambda}^T \mathbf{A}_t \boldsymbol{\lambda} - \mathbf{b}_t^T \boldsymbol{\lambda}$. Using these definitions, Lemma 8.1, and $\mathbf{G}\mathbf{G}^T = \mathbf{I}$, we obtain

$$\|\mathbf{B}_t\| \leq 1 \text{ and } \|\boldsymbol{\ell}_t^+\| = 0, \tag{8.8}$$

where for any vector $\mathbf{v} = [v_i]$, \mathbf{v}^+ denotes the vector with the entries $v_i^+ = \max\{v_i, 0\}$. Moreover, it follows by Theorem 8.2 that for any $C \geq 2$ there are constants $a_{\min}^C > a_{\min}^C > 0$ such that

$$a_{\min}^C \leq \lambda_{\min}(\mathbf{A}_t) \leq \lambda_{\max}(\mathbf{A}_t) \leq a_{\max}^C \tag{8.9}$$

for any $t \in \mathcal{T}_C$. As above, we denote by $\lambda_{\min}(\mathbf{A}_t)$ and $\lambda_{\max}(\mathbf{A}_t)$ the extreme eigenvalues of \mathbf{A}_t . Our optimality result for a model semicoercive boundary variational inequality then reads as follows.

Theorem 8.3. *Let $C \geq 2$ denote a given constant, let $\{\boldsymbol{\lambda}_t^k\}$, $\{\boldsymbol{\mu}_t^k\}$, and $\{\varrho_{t,k}\}$ be generated by Algorithm 6.1 (SMALBE) for (8.7) with $\|\mathbf{b}_t\| \geq \eta_t > 0$, $\beta > 1$, $M > 0$, $\varrho_{t,0} = \varrho_0 > 0$, $\varepsilon > 0$, and $\boldsymbol{\mu}_t^0 = \mathbf{o}$. Let $s \geq 0$ denote the smallest integer such that $\beta^s \varrho_0 \geq M^2/a_{\min}$ and assume that Step 1 of Algorithm 6.1 is implemented by means of Algorithm 5.8 (MPRGP) with parameters $\Gamma > 0$ and $\bar{\alpha} \in (0, (a_{\max} + \beta^s \varrho_0)^{-1}]$, so that it generates the iterates*

$$\boldsymbol{\lambda}_t^{k,0}, \boldsymbol{\lambda}_t^{k,1}, \dots, \boldsymbol{\lambda}_t^{k,l} = \boldsymbol{\lambda}_t^k$$

for the solution of (8.7) starting from $\boldsymbol{\lambda}_t^{k,0} = \boldsymbol{\lambda}_t^{k-1}$ with $\boldsymbol{\lambda}_t^{-1} = \mathbf{o}$, where $l = l_{t,k}$ is the first index satisfying

$$\|\mathbf{g}^P(\boldsymbol{\lambda}_t^{k,l}, \boldsymbol{\mu}_t^k, \varrho_{t,k})\| \leq M \|\mathbf{B}_t \boldsymbol{\lambda}_t^{k,l}\| \tag{8.10}$$

or

$$\|\mathbf{g}^P(\boldsymbol{\lambda}_t^{k,l}, \boldsymbol{\mu}_t^k, \varrho_{t,k})\| \leq \varepsilon M \|\mathbf{b}_t\|. \tag{8.11}$$

Then for any $t \in \mathcal{T}_C$ and problem (8.7), an approximate solution $\boldsymbol{\lambda}_t^{k_t}$ which satisfies

$$\|\mathbf{g}^P(\boldsymbol{\lambda}_t^{k_t}, \boldsymbol{\mu}_t^{k_t}, \varrho_{t,k_t})\| \leq \varepsilon M \|\mathbf{b}_t\| \text{ and } \|\mathbf{B}_t \boldsymbol{\lambda}_t^{k_t}\| \leq \varepsilon \|\mathbf{b}_t\| \tag{8.12}$$

is generated at $O(1)$ matrix–vector multiplications by the Hessian of the augmented Lagrangian L_t for (8.7) and

$$\varrho_{t,k} \leq \beta^s \varrho_0.$$

Proof. Notice that we assume that the constant C is fixed, so all the assumptions of Theorem 6.11 (i.e., the inequalities (8.8) and (8.9)) are satisfied for the set of indices \mathcal{T}_C . Thus to complete the proof, it is enough to apply Theorem 6.11. \square

Since the cost of a matrix–vector multiplication by the Hessian of the augmented Lagrangian L_t is proportional to the number of the dual variables, Theorem 8.3 proves numerical scalability of Algorithm 6.1 (SMALBE) for (8.7) provided the inner bound constrained minimization is implemented by means of Algorithm 5.8 (MPRGP). The parallel scalability follows directly from the discussion at the end of Sect. 8.2. We shall illustrate these features numerically in the next section.

8.5 Numerical Experiments

In this section we illustrate numerical scalability of SMALBE Algorithm 6.1 on the class of problems arising from application of the TFETI method described above to our boundary variational inequality (8.1). The domain Ω was first partitioned into identical squares with the side

$$H \in \{1/2, 1/4, 1/8, 1/16\}.$$

The square subdomains were then discretized by regular grids with the discretization parameter $h = H/64$, so that the discretized problems have the primal dimension

$$n \in \{33282, 133128, 532512, 21300048\}$$

and the dual dimension

$$m \in \{258, 1545, 7203, 30845\}.$$

The computations were performed with the parameters

$$M = 1, \quad \varrho_0 = 30, \quad \Gamma = 1, \quad \text{and} \quad \varepsilon = 10^{-4}.$$

The stopping criterion was

$$\|\mathbf{g}_t^P(\boldsymbol{\lambda}^k)\| \leq 10^{-4} \|\mathbf{b}_t\| \quad \text{and} \quad \|\mathbf{B}_t \boldsymbol{\lambda}^k\| \leq 10^{-4} \|\mathbf{b}_t\|.$$

Algorithm 6.1 with the solution of auxiliary bound constrained problem by Algorithm 5.8 was implemented in C exploiting PETSc [7]. Using Theorem 8.3, we get that the number of iterations that are necessary to find the approximate solution is bounded provided H/h is bounded. The solution for $H = 1/4$ and $h = 1/4$ is in Fig. 8.4.

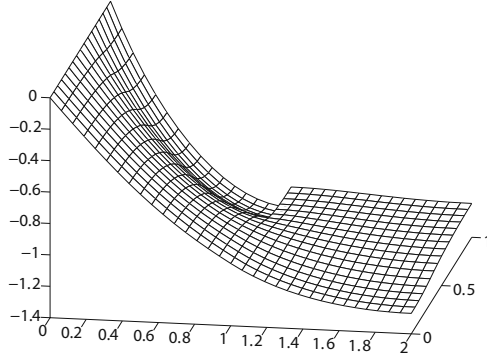


Fig. 8.4. Solution of the model semicoercive problem

The results of computations are in Fig. 8.5. We can see that the numbers of the conjugate gradient iterations (on vertical axis) which correspond to $H/h = 64$ vary very moderately with the dimension of the problem in agreement with Theorem 8.3, so that the cost of computations increases nearly linearly. The algorithm shares its parallel scalability with FETI; see, e.g., Dostál and Horák [64]. We conclude that it is possible to observe numerical scalability and that SMALBE with the inner loop implemented by MPRGP can be an efficient solver for semicoercive variational inequalities.

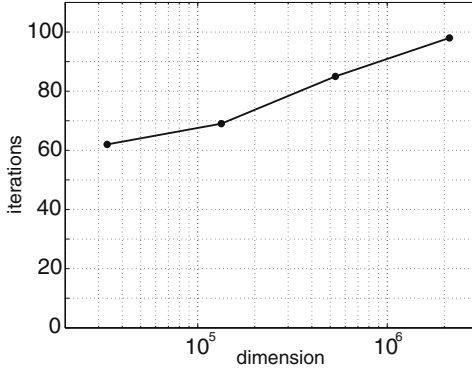


Fig. 8.5. Scalability of SMALBE with TFETI for the semicoercive problem with $H/h = 64$

More results of numerical experiments can be found in Dostál [49]. See also Dostál and Horák [64]. Applications to the contact problems of elasticity are in Dostál et al. [76].

8.6 Comments and References

For solvability and approximation theory for semicoercive variational inequalities see the references in Sect. 7.5. See also Proposition 2.16.

The linear augmented Lagrangians were often used in engineering algorithms to implement active constraints as in Simo and Laursen [167]. The first application of the nonlinear augmented Lagrangians with adaptive precision control in combination with FETI to the solution of variational inequalities and contact problems seems to be in Dostál, Friedlander, and Santos [55] and Dostál, Gomes, and Santos [60, 61]. Applications to 3D frictionless contact problems with preconditioning of linear step are, e.g., in Dostál et al. [53] and Dostál, Gomes, and Santos [59, 62]. Experimental evidence of scalability of the algorithm with the inner loop implemented by the proportioning [42] was given in Dostál and Horák [64]. Applications to the contact shape optimization are, e.g., in Dostál, Vondrák, and Rasmussen [77].

The method presented in this chapter solves both coercive and semicoercive problems. Our first proof of numerical scalability of an algorithm for the solution of a semicoercive variational inequality used the optimal penalty in dual FETI problem [65]. Optimality of outer loop was proved in Dostál [67]; the theory was completed in Dostál [48]. In particular, it was proved that the relative feasibility error of the solution of the FETI problem with a given penalty parameter can be bounded independently of the discretization parameter. The results presented here for a scalar semicoercive variational inequality can be extended, including the theoretical results, to the solution of 2D or 3D multibody contact problems of elasticity, including 2D problems with a given (Tresca) friction [63] and an approximation of 3D ones [69]. The scalability was proved also for the problems discretized by the BETI (boundary element tearing and interconnecting) method of Langer and Steinbach [141]; see Bouchala, Dostál, and Sadowská [18, 17, 19]. See also Sadowská [164].

There is an interesting corollary of our theory. If we are given a class of contact problems which involves bodies of comparable shape, so that the regular part of their spectrum is contained in a given positive interval, then Theorem 8.3 implies that *there is a bound, independent of a number of the bodies, on the number of iterations that are necessary to approximate the solution to a given precision*. The linear auxiliary problems can be preconditioned by the FETI preconditioners. For comprehensive review of domain decomposition methods with many references see, e.g., Toselli and Widlund [175].

Some methods reported in Sect. 7.5 can be naturally adopted for the solution of semicoercive problems. This concerns especially the active set-based algorithms with multigrid solvers of linear problems (see, e.g., Krause [134]) and the algorithm proposed by Schöberl. A FETI-based algorithm for coercive and semicoercive contact problems was proposed by Dureisseix and Farhat [78]. These authors gave experimental evidence of scalability of their algorithms.